

ULTRAVIOLET SUNSCREENS IN *GYMNODINIUM SANGUINEUM* (DINOPHYCEAE): MYCOSPORINE-LIKE AMINO ACIDS PROTECT AGAINST INHIBITION OF PHOTOSYNTHESIS¹

Patrick J. Neale,² Anastazia T. Banaszak, and Catherine R. Jarriel

Smithsonian Environmental Research Center, P.O. Box 28, Edgewater, Maryland 21037

ABSTRACT

Marine phytoplankton are sensitive to inhibition of photosynthesis by solar ultraviolet (UV) radiation, although sensitivity varies, depending on the growth environment. A mechanism suggested to increase resistance to UV inhibition is the accumulation of UV-absorbing compounds, such as the mycosporine-like amino acids (MAAs) found in many marine organisms. However, the effectiveness of these compounds as direct optical screens in microorganisms has remained unclear. The red-tide dinoflagellate *Gymnodinium sanguineum* Hirasaka accumulates about 14-fold more MAAs (per unit of chlorophyll) in high ($76 \text{ W}\cdot\text{m}^{-2}$) than in low ($15 \text{ W}\cdot\text{m}^{-2}$) growth irradiance. Biological weighting functions were estimated for UV inhibition of photosynthesis and showed that the high-light-grown cultures have lower sensitivity to UV radiation at wavelengths strongly absorbed by the MAAs. The time course of photosynthesis during exposure to UV radiation was measured using pulsed amplitude modulated (PAM) fluorometry and displayed a steady-state level after 15 min of exposure, indicating active repair of damage to the photosynthetic apparatus. Repair was blocked in the presence of the antibiotic streptomycin, yet high-light *G. sanguineum* remained less sensitive to UV radiation than did low-light cultures. These experiments show that MAAs act as spectrally specific UV sunscreens in phytoplankton.

Key index words: biological weighting function; dinoflagellate; fluorescence; photoinhibition; photoprotection; photosystem II; quantum yield

Abbreviations: BWF, biological weighting function; chl, chlorophyll a; P-I, photosynthesis vs. irradiance; PSII, photosystem II

Solar ultraviolet (UV, 290–400 nm) radiation affects phytoplankton growth and survival in near-surface waters by the inhibition of photosynthesis (Smith et al. 1980, Helbling et al. 1992, Smith et al. 1992), damage to DNA (Karentz et al. 1991a, Buma et al. 1995), and effects on other processes (Holm-Hansen et al. 1993). Concern about stratospheric ozone depletion and the associated enhancement of middle ultraviolet (UVB, 290–320 nm) has motivated spectral assessments of UV inhibition of photosynthesis to distinguish effects by UVB compared to the near ultraviolet (UVA, 320–400 nm), which is unaffected by ozone depletion (Cullen et al. 1992, Lubin et al. 1992, Neale et al. 1994, Boucher and

Prézelin 1996a, Neale et al. 1998a). Equally important, although less well understood, are protective mechanisms by which phytoplankton offset the negative effects of UV exposure (Vincent and Roy 1993). These mechanisms include protective processes that decrease the biological effectiveness of UV exposure and counteract processes, such as repair, reactivation, and protein turnover, that restore functions lost because of UV damage. Understanding such mechanisms is critical to assessing the long-term effect of changes in incident solar UV radiation on ecosystem processes (Bothwell et al. 1993).

One possible mechanism of increased protection from UV radiation is the accumulation of UV-absorbing compounds, or putative “sunscreens” (Vincent and Roy 1993). The mycosporine-like amino acids (MAAs) are a class of about a dozen related UV-absorbing compounds that are widespread in marine organisms (Carreto et al. 1990a, Karentz et al. 1991b, Shick et al. 1992, Stochaj et al. 1994, Banaszak and Trench 1995, Dunlap and Shick 1998). MAAs have sharp (ca. 20-nm-bandwidth) absorption peaks varying between 300 and 360 nm (Carreto et al. 1990a, Karentz et al. 1991b, Shick et al. 1992, Stochaj et al. 1994). Accumulation of MAAs is correlated with exposure to UV radiation in many marine organisms, so their protective function has been suggested for some time (Shibata 1969, Yentsch and Yentsch 1982, Dunlap et al. 1986, Vernet et al. 1989, Carreto et al. 1990a, Vernet et al. 1994, Banaszak and Trench 1995, Helbling et al. 1996). However, the efficiency and mode of protection of MAAs is not well understood. Some studies have suggested that the presence of MAAs does not necessarily result in photoprotection. The colonial form of an Antarctic prymnesiophyte, *Phaeocystis antarctica*, accumulates MAAs; however, growth of this alga has been reported to be sensitive to UVB (Karentz 1994, Karentz and Spero 1995; see contrasting results of Davidson et al. 1996). Moreover, some species of Antarctic diatoms do not accumulate MAAs yet survive UVB exposure better than *P. antarctica* (Davidson et al. 1994, Davidson and Marchant 1994). Optical models indicate that MAAs might not be an effective sunscreen over the short path lengths characteristic of phytoplankton cells (Garcia-Pichel 1994). Previous attempts to directly measure a “sunscreen factor” for MAAs have revealed only small (around 10%) increases in spectral filtering (Garcia-Pichel et al. 1993) and no significant decreases in UV biological weight (Lesser 1996a, b). MAAs do

¹ Received 6 April 1998. Accepted 1 September 1998.

² Author for reprint requests; e-mail neale@serc.si.edu.

protect against UV-induced developmental delays in the eggs of laboratory-reared green sea urchins, supporting a direct photoprotective role (Adams and Shick 1996). However, these authors also recognized that other mechanisms of MAA action might have provided protection (i.e. through antioxidant activity) (Dunlap and Yamamoto 1995).

Our experimental objective was to determine whether MAAs act as a direct, spectral screen against solar UV exposure in marine microorganisms. We quantitated the protective function of MAAs in a marine dinoflagellate as the increased resistance to inhibition of photosynthesis by UV radiation in the wavelength band absorbed by the MAAs. The spectral dependence of inhibition was described by a biological weighting function, or BWF (Cullen and Neale 1997). A BWF is similar to an action spectrum, the difference being that it is inferred from polychromatic exposures, as is appropriate for processes, such as photosynthesis, that respond to multiple wavebands (Coochill 1991). Previous work has shown that photosynthesis as a function of UV and photosynthetically available radiation (PAR, 400–700 nm) is well described by a model, the BWF/P-I model, which combines the BWF with a saturating function of PAR irradiance (Cullen et al. 1992, Neale et al. 1994, Neale et al. 1998a). We examined the responses of *Gymnodinium sanguineum* Hirasaka, which can form extensive surface blooms (“red tides”) in marine coastal and estuarine waters, such as the Chesapeake Bay.

MATERIALS AND METHODS

Culture growth conditions. We used a clone of *G. sanguineum*, isolated by D. Wayne Coats from the Rhode River, a subestuary of the Chesapeake Bay, and grown under low light (LL) and high light (HL). Cultures were grown under cool-white fluorescent lights on a 14:10 h LD cycle at 25°C. The growth medium was a standard “f/2” enrichment of filtered seawater from the Gulf Stream diluted to 15‰. The scalar irradiance in the growth flasks was 15 W·m⁻² of PAR (LL) and 76 W·m⁻² (HL). Light measurements were made with a quantum scalar (4π) sensor (Biospherical Instruments QSL-100) positioned in the center of a 250-mL growth flask filled with media and converted to PAR irradiance in energy units (W·m⁻²) by application of a conversion factor (4.6 μmol·J⁻¹) determined from measured spectral irradiance of the fluorescent lights. Cultures were maintained in exponential growth in each light regime with biweekly transfers for at least 2 months before the first experiment.

Photosynthetic response to UV. The dependence of photosynthesis on PAR and inhibition by UV radiation was measured as the uptake of H¹⁴CO₃⁻ in organic compounds during a 1-h exposure in a special spectral incubator, the photoinhibitor, which provides PAR and UV irradiance of varying intensity and polychromatic spectral composition. The incubator uses a 2500-W xenon lamp, which illuminates a temperature-controlled block with 72 positions for 1-cm-diameter cuvettes with flat quartz bottoms. Irradiance from the lamp is reflected by a mirror to illuminate culture aliquots (1 mL) through the bottom of the cuvette after passing through a series of filters as follows: (1) a water heat-trap, (2) one of seven Schott WG series long-pass filters (280, 295, 305, 320, 335, 345, and 360) or a GG400 filter that excludes all UV, and (3) within each spectral filter, neutral density screens so as to obtain nine intensities. The numerical suffix of each filter denotes an approximate wavelength of 50% transmission, declining to 0% at shorter wavelengths. Spectral irradiance for each treat-

ment (and other irradiance sources) was measured (0.2-nm resolution) with a specially configured quartz fiber-optic and diode-array spectroradiometer (Cullen and Lesser 1991) that was calibrated with a NIST-traceable 1000-W lamp (Eppley FEL) supplied with constant current by a HP6030A power supply. Further details on the spectroradiometer and incubator are given in Cullen et al. (1992), Neale et al. (1994), and Neale et al. (1998a). Biological weighting functions were estimated from the measured rates using statistical methods as previously described (Cullen et al. 1992, Cullen and Neale 1997). Briefly, the data are fit to the following equation:

$$P^B = P_s^B \tanh(E_{\text{PAR}}/E_s) \left(\frac{1}{1 + E_{\text{inh}}^*} \right) \quad (1)$$

where P^B is photosynthesis normalized to chl *a* content (gC·gchl⁻¹·h⁻¹), P_s^B is the saturated rate of photosynthesis in the absence of inhibition, and E_s is a saturation parameter for PAR irradiance (E_{PAR} , W·m⁻²). A dimensionless inhibition index, E_{inh}^* , is defined as

$$E_{\text{inh}}^* = \sum_{\lambda=280\text{nm}}^{400\text{nm}} \varepsilon(\lambda) \cdot E(\lambda) \cdot \Delta\lambda \quad (2)$$

where $\varepsilon(\lambda)$ is biological weight (reciprocal mW·m⁻²) at wavelength λ and $E(\lambda)$ is spectral irradiance at λ (mW·m⁻²·nm⁻¹). A detailed protocol is given by Cullen and Neale (1997). This implementation differed from that previously described (Cullen et al. 1992) in using the hyperbolic tangent (tanh) function for the P-I response, which improved the fit. BWFs were independently estimated for separate trials (five in high light, four in low light). The mean BWF for each light regime was also calculated, with confidence intervals for the mean derived from individual error estimates by propagation of errors (Bevington 1969).

More detailed P-I curves for PAR-only exposure were obtained in separate “photosynthetic” incubations using a modification of the protocol described by Lewis and Smith (1983). Aliquots of culture (1 mL) were incubated in 7-mL scintillation vials under 37 light levels that were obtained by filtering irradiance from a 250-W halogen lamp with neutral density screens. Irradiance was measured with a quantum scalar sensor (QSL-100) mounted inside a scintillation vial. Quantum scalar irradiance (μmol·m⁻²·s⁻¹) was converted to E_{PAR} (W·m⁻²) by application of a conversion factor (4.9 μmol·J⁻¹) determined from measured spectral irradiance. Photosynthetic parameters P_s^B and E_s were estimated by fitting the hyperbolic tangent curve as in Equation 1 (i.e. with $E_{\text{inh}}^* = 0$).

Cellular absorption and chlorophyll. Cells concentrated on glass fiber filters were scanned in a Cary 4 dual beam spectrophotometer, using a blank filter wetted with filtrate as a control. Spectra were corrected for path-length amplification as described (Cleveland and Weidemann 1993). Chlorophyll *a* concentration (chl) was measured fluorometrically on aliquots concentrated on glass fiber filters (Whatman GF/F) and extracted in 90% acetone for at least 24 h in the dark at 4°C.

Mycosporine-like amino acids. For all samples, the extraction and analysis of MAAs were performed as described (Dunlap and Chalker 1986) with minor modifications. Briefly, approximately 50 mL of sample water were filtered onto GF/F filters and frozen (-70°C) until analysis. Filters were extracted overnight in 1 mL of 100% high-performance liquid chromatography (HPLC)-grade methanol at 4°C; the extracts were centrifuged, and the supernatant was used for MAA analysis. Individual MAAs were separated by reverse-phase, isocratic HPLC on a Brownlee RP-8 column (Spheri-5, 4.6 mm ID × 250 mm), which was protected with an RP-8 guard column (Spheri-5, 4.6 mm ID × 30 mm). The mobile phase consisted of 25% methanol (v/v), 0.1% glacial acetic acid (v/v) in water with a flow rate of 0.7 mL·min⁻¹. Detection of the peaks was carried out using a diode array, UV absorbance detector (Beckman Gold System). Standards were available for seven MAAs (mycosporine-glycine, shinorine, porphyra-334, palythine, asterina-330, palythanol, and palythene). Standards were originally isolated by Walter Dunlap and were kindly provided by Deneb Karentz and Michael Lesser. Identities of peaks were con-

TABLE 1. Growth characteristics of *Gymnodinium sanguineum* cultures. Mean \pm standard deviations of replicate culture trials, $n = 5$ for high light (HL), and $n = 4$ for low light (LL).

	Growth rate (d ⁻¹)	Cell density (cells·mL ⁻¹)	Chl (μ g·L ⁻¹)	Cellular chl (pg·cell ⁻¹)
HL	0.23 \pm 0.04	2498 \pm 435	51 \pm 12	20.4
LL	0.15 \pm 0.02	826 \pm 151	63 \pm 16	76.3

firmed by co-chromatography with standards and by the maximal wavelength of absorbance by on-line diode array spectroscopy. All MAA concentrations are expressed in nmol (nmol chl)⁻¹.

Photochemical efficiency of photosystem II. A pulse amplitude modulated (PAM) fluorometer (Walz, Effeltrich, Germany) was used with a high-sensitivity detector as described (Schreiber 1994). One milliliter of culture was placed in a 1-cm-square quartz cuvette. The cuvette was illuminated from below using irradiance from a 150-W xenon lamp (Schoeffel) filtered through selected Schott long-pass filters. The fluorometer measures the steady-state *in vivo* chl fluorescence (F_s) of phytoplankton during illumination with actinic irradiance. At 1-min intervals a saturating flash (400-ms pulse duration) was applied to obtain a maximum yield (F'_m). The relative efficiency of excitation energy capture by photosystem II (ψ_{PSII}) is calculated as $(F'_m - F_s)/F'_m$. Active fluorescence measurements of ψ_{PSII} have been shown to be highly correlated with the overall efficiency (ψ_p) and, thus, rate of photosynthesis (Genty et al. 1989). For each sample, there was an initial 10-min period without actinic illumination to measure maximum ψ_{PSII} , followed by illumination with PAR only (GG400 filter). During the initial few minutes of steady PAR illumination, ψ_{PSII} displayed short-term variations consistent with the activation of photosynthesis, but after 10 min, ψ_{PSII} was nearly constant (Schreiber et al. 1986). Once steady-state ψ_{PSII} was reached, kinetics of UV effects were observed through the decrease in ψ_{PSII} upon supplementing

the PAR illumination with UV. In some cases, a streptomycin solution in distilled water (final concentration 250 μ g·mL⁻¹ [Stein 1973]) was added after 10 min of PAR exposure, followed by another 10 min of PAR exposure before UV exposure began.

RESULTS AND DISCUSSION

The initial density of the *G. sanguineum* cultures after biweekly transfer was 100 cells·mL⁻¹. Experiments were performed 11 days after transfer for HL cultures and 12 days after transfer for LL cultures (Table 1). *Gymnodinium sanguineum* grew 57% faster in HL compared to LL, and cell density of samples used for photosynthesis measurements was three times higher in HL. In contrast, the chl concentration was slightly higher in the LL cultures because of the much higher cellular chl content (Table 1). Growth in LL was limited by light, and *G. sanguineum* acclimated through the accumulation of photosynthetic pigments (Richardson et al. 1983, Falkowski and LaRoche 1991).

Photosynthesis. Estimates for the parameters of PAR-dependent photosynthesis were obtained by fitting Equation 1 to observations of carbon assimilation in the photosynthetron (halogen lamp) and during exposure to the xenon lamp (an example data set is shown in Fig. 1). Analysis of the photosynthetron results showed that E_s was significantly (ca. 30%) lower in LL cultures. Also, P_s^B was slightly (ca. 6%) higher in LL cultures (Table 2), but the difference was not very significant ($P > 0.05$). Anal-

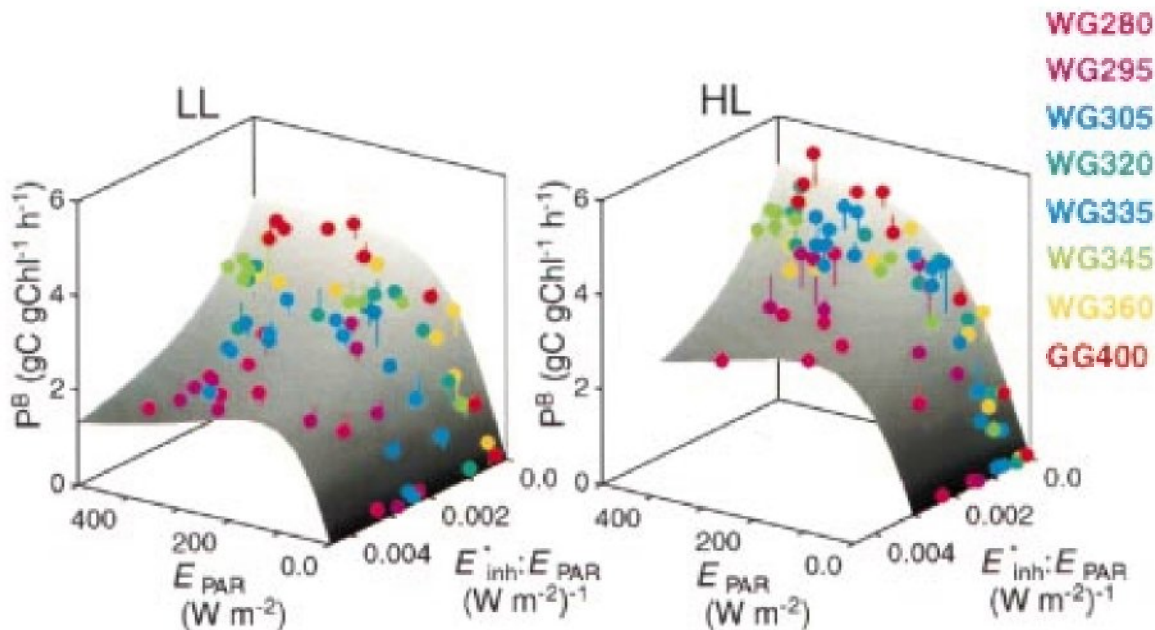


FIG. 1. Photosynthetic rates P^B ($\text{gC}\cdot\text{gchl}^{-1}\cdot\text{h}^{-1}$) of LL and HL cultures of *G. sanguineum* in a spectral incubator versus PAR in $\text{W}\cdot\text{m}^{-2}$ (E_{PAR}) and the ratio ($E_{\text{inh}}^* : E_{\text{PAR}}$) of biologically weighted UV irradiance (E_{inh}^*) and PAR (ratio has units of reciprocal $\text{W}\cdot\text{m}^{-2}$). Treatments with the same spectral filter have the same color symbol, ranging from red for the 400-nm long-pass filter (GG400) to violet for the 280-nm long-pass filter (WG280). Treatments in the same filter type have about the same $E_{\text{inh}}^* : E_{\text{PAR}}$; variability of the ratio is due to spatial differences in the xenon lamp spectrum. The shaded surface shows predicted rates of photosynthesis by the fitted BWF/P-I model. The fitted BWF was also used to estimate E_{inh}^* for each treatment. The magnitude and direction of the difference between predicted and fitted is shown by the line segment projecting from the symbol. These are the results for one set of HL and LL cultures; similar responses were obtained in four other trials of HL and three other trials of LL cultures.

TABLE 2. Photosynthetic parameters estimated for *G. sanguineum* cultures grown in high light (HL, five trials) and low light (LL, four trials). Mean \pm standard error of estimates for the saturated rate of photosynthesis in absence of photoinhibition (P_s^B , mg C [mg chl] $^{-1}$ ·h $^{-1}$) and light saturation parameter (E_s , W·m $^{-2}$). Estimates were obtained using the photosynthetron data fitted to a hyperbolic tangent curve ($n = 37$ per curve) and the photoinhibitor data fitted to the BWF/P-I model ($n = 72$ per curve). Further details on measurement conditions and parameter estimation are given in Materials and Methods.

		P_s^B (mg C [mg chl] $^{-1}$ ·h $^{-1}$)	E_s (W·m $^{-2}$)	R 2
P-I	HL	6.47 \pm 0.16	113 \pm 8	0.98
	LL	6.83 \pm 0.11	78 \pm 4	0.98
BWF/P-I	HL	4.19 \pm 0.86	140 \pm 34	0.92
	LL	4.78 \pm 0.82	115 \pm 21	0.92

ysis of PAR-dependent photosynthesis in the photoinhibitor (cf. Fig. 1, GG400 filter) also indicated that photosynthesis by cultures grown in LL saturated at lower irradiance (E_s) and attained a higher rate per unit chl at saturation. However, in this case the differences in parameter estimates were not statistically significant ($P > 0.05$, t -test). The statistical resolution for P-I parameters was less than for the photosynthetron because most of the statistical power in the photoinhibitor design is directed toward resolving spectral responses.

The differences in PAR-dependent photosynthesis between the HL and the LL culture support the conclusion that acclimation to growth-limiting irradiance was occurring in the LL cultures. The capacity for photon capture increased in the LL cultures, as has been observed for other phytoplankton (Richardson et al. 1983, Falkowski and LaRoche 1991). The slight decrease of P_s^B in HL cultures might be due to higher respiration rates in the light (Kana 1990).

Although the relative differences between HL and LL were the same in the photoinhibitor and photosynthetron results, the photosynthetic parameters were different. The values of E_s were lower under the halogen lamp irradiance of the photosynthetron. This is presumably because of the more efficient utilization of the red-enriched irradiance of the photosynthetron (cf. Vernet et al. 1989). The difference remained even after adjusting for the 11% lower photon content of xenon versus halogen irradiance. Interestingly, estimates of P_s^B were consistently higher under halogen lamp exposure than under xenon lamp exposure. This effect was not due to differences in incubation temperature, which was measured to be 24.6°C \pm 0.3°C in each case. Qualitatively similar differences have been observed in a wide range of samples (Neale and Banaszak, unpubl.) and might be due to chromatic regulation of P_s^B . The spectral characteristics of the response are presently under study.

Under exposure to UV irradiance in the photoinhibitor, LL cultures had greater relative decrease in P_s^B than HL cultures receiving the same irradi-

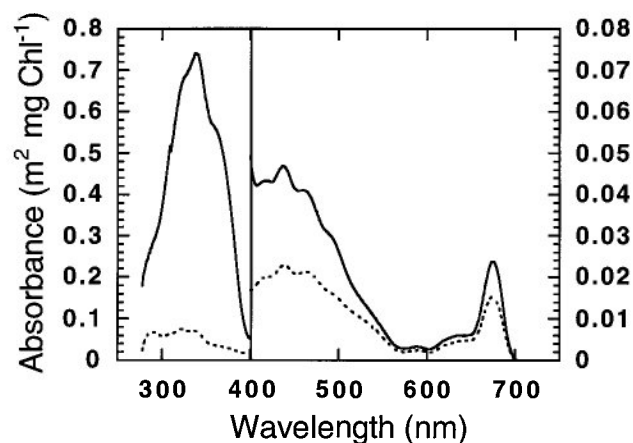


Fig. 2. Average spectral absorbance (a_{ph}^* , m 2 mg·chl $^{-1}$) by *G. sanguineum* cultures for high-growth irradiance (HL, solid line, $n = 5$) and low-growth irradiance (LL, dashed line, $n = 4$). The maximum y for the UV portion of the spectrum (left scale) is 10 times greater scale than the visible (right scale). The prominent peak in the 320–360-nm region is due to MAA absorbance.

ance, indicating an increased resistance to UV radiation in the HL cultures (Fig. 1). In addition, the decreased sensitivity of HL cultures was spectrally variable. Light treatments with mainly longer-wavelength UVA (360-nm, 345-nm, and 335-nm long-pass filters) had little effect on photosynthesis by HL cultures, but these cultures were sensitive to treatments with short-wavelength UVB (280-nm, 295-nm, and 305-nm long-pass filters) (Fig. 1). In contrast, the LL cultures were broadly sensitive to both UVA and UVB irradiance.

Spectral absorption. Light absorption by the HL and LL cultures differed in both the PAR and the UV range. Absorption of PAR per unit chl was greater in the HL cultures (Fig. 2), probably because of pigment self-shading, or the “packaging” effect, in the LL culture. The difference is even more dramatic in the UV, where absorption per unit chl was about six times higher in the HL cultures than in the LL cultures (Fig. 2).

Analysis of cell extracts revealed that the increased absorbance was due to the presence of MAAs, which were found in about 14-fold higher concentration in the HL cultures when normalized to chl content (Table 3). High concentrations of UV-absorbing compounds have been observed in several species of bloom-forming dinoflagellates that, by accumulating in surface waters, are exposed to HL conditions (Yentsch and Yentsch 1982, Balch and Haxo 1984, Vernet et al. 1989, Carreto et al. 1990b). Carreto et al. (1989) showed that transferring cultures of the red-tide dinoflagellates *Alexandrium excavatum* and *Prorocentrum micans* from low (20 μ mol quanta·m $^{-2}$ ·s $^{-1}$) to high (250 μ mol quanta·m $^{-2}$ ·s $^{-1}$) light intensity resulted in a rapid increase in the content of UV-absorbing compounds as determined by the ratio of 365:672 nm absorption. This process was reversible in both species. Sev-

TABLE 3. Average concentration of mycosporine-like amino acids (MAAs, $\text{nmol} \cdot [\text{nmol chl } a]^{-1}$) in *G. sanguineum* grown under high light (HL) and low light (LL). Mean of five replicate cultures grown under each regime, \pm standard error. The ratio of the concentrations HL to LL is also given. Four MAAs were detected, and wavelengths of peak absorbance in methanol are given in parentheses.

	Mycosporine-glycine (310 nm)	Palythine (320 nm)	Porphyra-334 (334 nm)	Palythene (360 nm)
HL	7.12 ± 0.57	0.66 ± 0.25	9.10 ± 0.28	27.47 ± 0.90
LL	0.53 ± 0.09	0.05 ± 0.02	0.83 ± 0.10	0.68 ± 0.09
Ratio HL:LL	13.5	6.2	13.3	14.8

en different MAAs were later identified (Carreto et al. 1990b) in *A. excavatum*, four of which are found in *G. sanguineum* under our culture conditions (Table 3). *Prorocentrum micans* in culture also contained a complex of seven MAAs (Carreto, unpubl., in Carreto et al. 1990), whereas Lesser (1996a) reported four MAAs in the same species. *Amphidinium carterae* differs from other species of dinoflagellates in not accumulating high amounts of MAAs even under UV exposure (Hannach and Sigleo 1998). The only other dinoflagellate in culture with identified MAAs to date is *Symbiodinium microadriaticum*, the symbiont of *Cassiopeia xamachana* (Banaszak and Trench 1995). In laboratory experiments, greater concentrations of three MAAs (mycosporine-glycine, shinorine, and porphyra-334) were produced by *S. microadriaticum* in the presence of UV radiation and PAR than in the presence of PAR only ($80 \mu\text{mol quanta} \cdot \text{m}^{-2} \cdot \text{s}^{-1}$) treatments. Whether high levels of PAR would induce the production of MAAs in the absence of UV radiation was not tested. No MAAs were induced in a closely related species, *S. californium*, the symbiont of *Anthopleura elegantissima*,

grown in the same light regimes (Banaszak and Trench 1995).

Several species of Antarctic diatoms also exhibit variations in MAAs in response to increased UV (Vilafañe et al. 1995, Riegger and Robinson 1997) or HL (UV and PAR) conditions (Helbling et al. 1996). Helbling et al. (1996) showed that two species of centric diatoms, *Thalassiosira* sp. and *Corethron criophilum*, which had been growing in culture at $250 \mu\text{mol quanta} \cdot \text{m}^{-2} \cdot \text{s}^{-1}$, increased MAA concentration in response to exposure to natural solar radiation (ranging from 340 to $1320 \mu\text{mol quanta} \cdot \text{m}^{-2} \cdot \text{s}^{-1}$, depending on species and day of experiment). In contrast, two species of pennate diatoms, *Pseudonitzschia* sp. and *Fragilariopsis cylindrus*, which had much lower MAA concentrations compared to the centric diatoms, increased MAA production only in the presence of UV radiation. The bloom-forming prymnesiophyte *Phaeocystis pouchetii* produces UV-absorbing compounds in response to exposure to UVB radiation and might provide UV protection for organisms present in the water column during a *P. pouchetii* bloom (Marchant et al. 1991).

Biological weighting functions. Four estimates of the BWF for inhibition of photosynthesis by UV radiation were obtained for each culture trial using from one to four spectral components as previously described (Neale et al. 1994, Cullen and Neale 1997). Increasing the number of components in the estimation of the BWF allows greater complexity of the spectral shape. However, additional components are accepted in the estimate only to the extent that they significantly increase variance explained by the BWF/P-I model (sequential *F*-test). For the LL cultures, two spectral components were sufficient to obtain maximum variance explained (R^2); that is, no significant increase in R^2 occurred when a third component was added to the fit (mean $F_{1,70} = 0.99$, $P > 0.25$). Consistent with this result, there were no differences in the shapes of the BWFs for LL cultures estimated with two or three components. In contrast, incorporating a third component did increase R^2 for the HL cultures (mean $F_{1,70} = 9.99$, $P < 0.05$), indicating an inherently more complex shape. Incorporating a fourth component did not significantly increase R^2 in either the LL or the HL culture trials.

Estimated weights were similar for the four trials conducted with LL-grown cultures (Fig. 3). In all

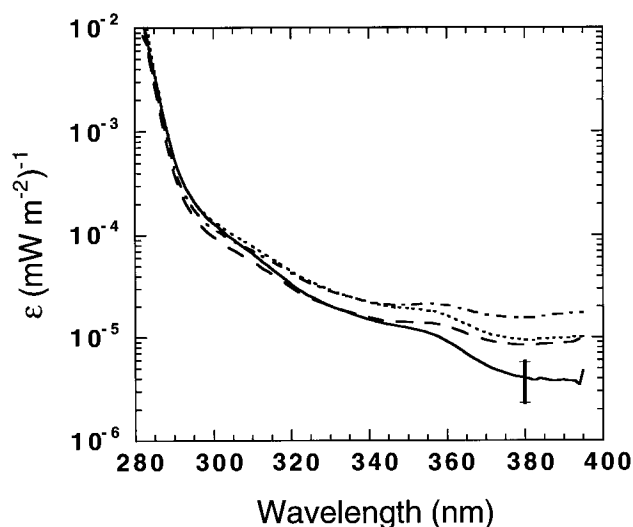


Fig. 3. Biological weight for the inhibition of photosynthesis by UV ($\epsilon[\lambda]$, reciprocal $\text{mW} \cdot \text{m}^{-2}$) estimated by statistical analysis of data from LL cultures. Independent estimates from four trials are shown. The solid line shows the weights estimated using the LL data in Figure 1. The vertical bar shows the average 95% confidence interval as a proportion of the estimate over all four curves. The solid line is at the midpoint of the interval, which is arithmetically symmetrical around the estimate.

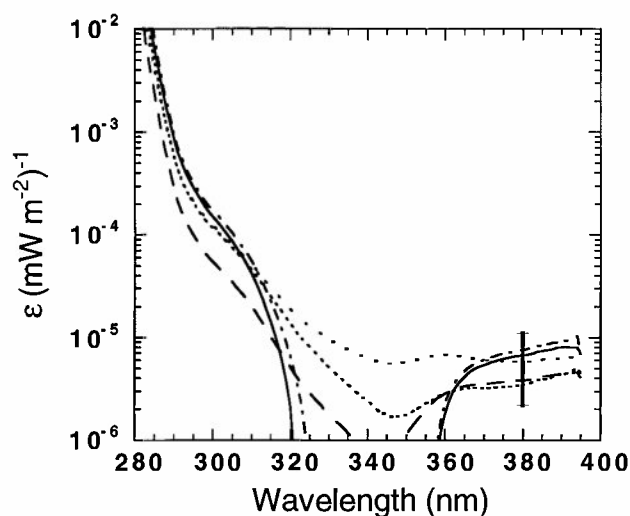


Fig. 4. Biological weight for the inhibition of photosynthesis by UV ($\epsilon[\lambda]$, reciprocal $\text{mW}\cdot\text{m}^{-2}$) estimated by statistical analysis of data from HL cultures. The solid line shows the BWF estimated using the HL data shown in Figure 1. The vertical bar shows the average 95% confidence interval as a proportion of the estimate over all five curves, excluding the wavelength interval between 320 and 360 nm. The solid line is at the midpoint of the interval, which is arithmetically symmetrical around the estimate. In the 320–360-nm interval, the estimate was near zero, so a proportional error estimate was not calculated. Weights $< 10^{-6}$ were not plotted. The average confidence interval in this region was $\pm 5.7 \times 10^{-6}$.

cases, there was significant weight for inhibition of photosynthesis by UV radiation ($\epsilon[\lambda]$, reciprocal $\text{mW}\cdot\text{m}^{-2}$) across the spectrum. Damaging potential decreased with an approximately exponential slope as a function of increasing wavelength. There was some variation in biological weight at the longer wavelengths; however, the variation between cultures was not significant.

The BWFs for the HL-grown cultures had more complicated shapes and were more variable between trials (Fig. 4). Weights were especially variable in the spectral range of 320–360 nm, in which the UV response was consistent with much lower biological weights compared to LL-grown cultures. In some cases, estimated weights were slightly positive and in others slightly negative. Negative weights occur when the beneficial effects of irradiance at a wavelength (i.e. as an energy source for photosynthesis or an inducer of repair) outweigh the damaging effects. However, the 95% confidence interval for all estimates in the 320–360-nm region overlapped zero, except for the BWF with the most positive $\epsilon(\lambda)$, which had a 95% confidence interval overlapping zero in the 330–350-nm region.

The average BWF for HL and LL cultures over all trials for each culture regime is shown in Fig. 5. A 95% confidence interval for the mean weight was calculated by propagation of errors from the individual estimates (Bevington 1969). The greatest difference between HL and LL $\epsilon(\lambda)$ is over the 325–

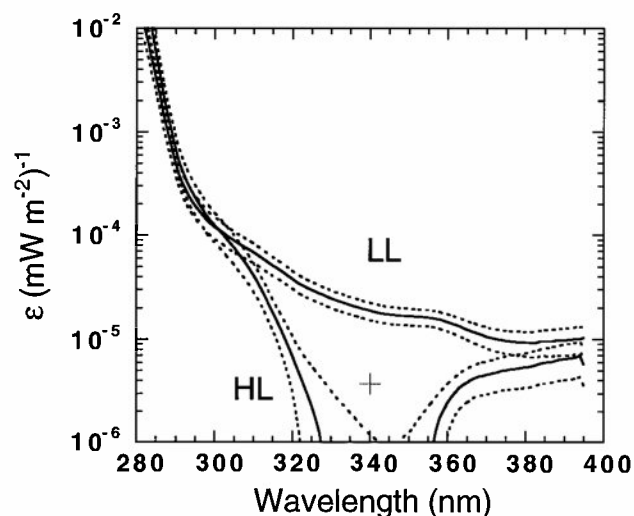


Fig. 5. Average biological weight for the inhibition of photosynthesis by UV ($\epsilon[\lambda]$, reciprocal $\text{mW}\cdot\text{m}^{-2}$, $n = 5$) for all curves shown in Figures 3 and 4. The solid line is the estimated average $\epsilon(\lambda)$; flanking dashed lines delimit the range of the 95% confidence interval for the mean estimate. Average curves for the high-growth irradiance (HL) and low-growth irradiance (LL) cultures are shown. For the HL culture in the 325–355-nm region, the 95% confidence interval for the mean overlaps zero, therefore these values were omitted from this logarithmic scale plot. The cross indicates the weight at 340 nm that would be obtained by applying a sunscreen factor (S) of 0.8 to the biological weight at 340 nm for LL cultures ($\epsilon_{\text{LL}}[340]$).

355-nm range. Exposure to these wavelengths significantly inhibited photosynthesis in LL cultures; however, the $\epsilon(\lambda)$ of HL cultures could not be statistically distinguished from zero. Outside this waveband (i.e. at both lower and higher wavelengths), the UV sensitivity of the HL culture approached that of the LL culture. The shape of the HL spectrum strongly supports the conclusion that MAAs provide direct photoprotection to the *G. sanguineum* cells. The greatest difference between the HL and the LL BWFs is for the 320–360-nm region (Fig. 6). The shape of the LL-HL difference spectrum is very similar to the wavelength band of largest enhancement of intracellular UV absorbance in the HL culture compared to the LL culture (Fig. 2). The decrease in sensitivity of the HL culture is especially dramatic for the spectral region in which solar radiation most inhibits photosynthesis in the LL culture (maximum of the product $\epsilon_{\text{LL}}[\lambda] \cdot E[\lambda]$) (Fig. 6). This indicates that MAAs are specifically accumulated to provide spectral protection against solar UV.

Repair. Our results, showing that MAAs produce a spectrally specific feature in the BWF, are persuasive support for the hypothesis that MAAs act as potent UV “sunscreens” in phytoplankton. The spectral difference between HL and LL BWFs strongly suggests that accumulation of MAAs accounts for the increased resistance to UV radiation acquired by HL cultures. However, organisms have multiple defenses against UV. Biological weighting functions (un-

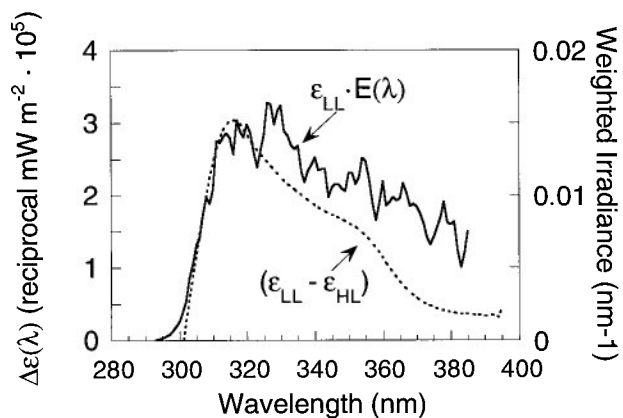


Fig. 6. Difference between the average $\varepsilon(\lambda)$ of the LL culture and HL culture ($\varepsilon_{LL}[\lambda] - \varepsilon_{HL}[\lambda]$, reciprocal $\text{mW}\cdot\text{m}^{-2}$), which measures the decrease in sensitivity to UV (dashed line), compared to weighted irradiance for inhibition of photosynthesis in the LL culture ($\varepsilon_{LL}[\lambda]\cdot E(\lambda)$, nm^{-1} , solid line). Spectral irradiance is a midday measurement for near summer solstice at 40°N (Table Mountain, Colorado) with a total column ozone of 290 Dobson Units, reported by Early et al. (1998) and smoothed to 1 nm effective bandwidth before weighting.

like action spectra) are composite functions in which the weights include both the direct effect of a specific wavelength and interactive effects with other wavelengths (Coohill 1991). The interactive effect could be, for example, the induction of repair processes by UVA illumination (Hirosawa and Miyachi 1983, Greenberg et al. 1989). Thus, to better define the protective role of MAAs, we examined the extent to which HL cultures exhibited a greater resistance through processes that actively counteract UV damage during exposure. The presence of these opposing processes can be diagnosed from the time course of photosynthesis during UV treatment. A rapid decrease in photosynthetic rate, followed by stabilization of photosynthesis at a depressed but steady-state level, implies that damage is partially counteracted by ongoing repair of the target site(s) within the photosynthetic apparatus. We measured time courses of relative PSII efficiency (ψ_{PSII}) using active fluorometry, as previous studies have indicated that ψ_{PSII} is closely coupled to the quantum yield of photosynthesis (Genty et al. 1989). Thus, ψ_{PSII} should reflect damage and repair occurring anywhere in the photosynthetic apparatus, not only in PSII.

In time-series experiments with *G. sanguineum*, cultures were first exposed to a moderate level of PAR only ($160\text{ W}\cdot\text{m}^{-2}$ of xenon irradiance filtered by a 400-nm long-pass cutoff filter), after which UV radiation was added, while PAR was maintained constant, by exchanging the filter with a 305-nm long-pass cutoff filter. Upon illumination with this broad-spectrum UV+PAR, there was a small drop in PSII efficiency in HL cultures, whereas PSII efficiency decreased but reached a lower steady-state level after about 15 min in LL cultures (Fig. 7). The lower PSII

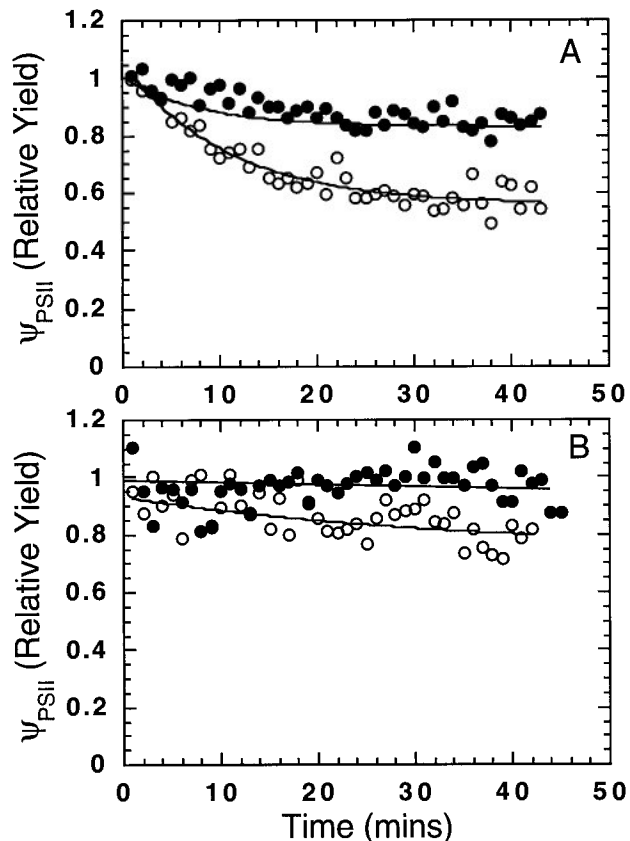


Fig. 7. Time course of the decrease in PSII efficiency (ψ_{PSII}) during UV exposure (xenon lamp and a 305-nm long-pass filter [WG305]) of (A) low-light-grown (LL) and (B) high-light-grown (HL) *G. sanguineum* cultures as monitored by PAM fluorometry. PSII efficiency ($\psi_{\text{PSII}} = [F'_m - F'_s]/F'_m$) was estimated from the steady-state (F'_s) and maximum (F'_m) fluorescence yields sampled at 1-min intervals (points). The ψ_{PSII} during the time course is plotted relative to the average ψ_{PSII} during a 10-min preexposure at the same PAR irradiance ($160\text{ W}\cdot\text{m}^{-2}$) but no UV (long-pass filter with 400-nm cutoff). Points were used to fit a curve for first-order kinetics using nonlinear regression (line). Measurements were made in absence (solid symbols) and presence (open symbols) of streptomycin ($250\text{ }\mu\text{g}\cdot\text{mL}^{-1}$). Maximum ψ_{PSII} (no actinic) for these runs was 0.56 (HL), 0.62 (HL + strep), 0.69 (LL), and 0.69 (LL + strep). Initial ψ_{PSII} in PAR was 0.29 (HL), 0.36 (HL + strep), 0.40 (LL), and 0.49 (LL + strep).

efficiency implies a lowering of photosynthetic rate. Indeed, the difference between HL and LL ψ_{PSII} is consistent with the difference in photosynthesis by HL and LL cultures, as predicted by the BWF/P-I model under the time-series experiment conditions (Figs. 1, 3, 4) (Lesser et al. 1994). Agreement between changes in ψ_{PSII} and predicted photosynthesis was also evident over a series of trials with both HL and LL cultures using a range of intensities and spectral treatments (data not shown). Steady-state ψ_{PSII} after UV treatment for these trials ($n = 13$) was on average 71% of initial yield; application of the corresponding BWFs predicted that photosynthesis under UV exposure in the PAM would be 66% of the PAR-only control.

The rapid attainment of a steady state suggests

that repair processes are partially counteracting UV damage and thus are an important factor in determining the overall response of dinoflagellates to UV. To determine the contribution of repair to the increased resistance observed in the HL cultures, cultures were treated with an inhibitor of chloroplast protein synthesis, streptomycin. This inhibitor limits repair capacity to the extent that damaged proteins cannot be restored to function through turnover processes (Samuelsson et al. 1985). Streptomycin was previously shown to enhance inhibition by UV radiation in a marine diatom (Lesser et al. 1994). After the addition of streptomycin, both HL and LL cultures were significantly more sensitive to UV radiation as evidenced by a greater decrease in PSII efficiency over the 45-min exposure (Fig. 7). Rates still approached a steady state; apparently, there was some residual repair capacity despite using the maximum recommended dose for algal cultures ($250 \mu\text{g}\cdot\text{mL}^{-1}$ [Stein 1973]). The important point is that streptomycin treatment did not narrow the difference in sensitivity between HL and LL cultures. On the contrary, the difference in PSII efficiency between HL and LL cultures after a 45-min exposure is actually larger in the presence of streptomycin. These time series indicate that repair processes are active in both cultures, but the capacity for repair is not markedly augmented in HL cultures. We conclude that the increased resistance of the HL cultures to UV radiation is primarily due to enhanced photoprotection by MAAs.

Comparison with previous results. The sunscreen potential of MAAs has been frequently suggested on the basis of the correlative evidence that organisms (algae and invertebrates) with higher concentrations of the compounds appeared to be more resistant to UV radiation (Yentsch and Yentsch 1982, Dunlap et al. 1986, Vernet et al. 1989, Carreto et al. 1990a, Karentz et al. 1991b, Shick et al. 1992, Stochaj et al. 1994, Vernet et al. 1994, Banaszak and Trench 1995, Helbling et al. 1996), but little optical evidence was available to define the specific function of MAAs (Garcia-Pichel et al. 1993, Garcia-Pichel 1994). Our results provide optical evidence that MAAs are direct protectants in *G. sanguineum* and possibly in other MAA-accumulating phytoplankton with a similar cell size as *G. sanguineum* (mean diameter $44 \mu\text{m}$ in the HL culture). In the absence of data showing that protection was targeted to the spectral region of greatest MAA absorbance, previous studies could not determine which portion of the increased resistance was due to the MAAs as opposed to other photoprotective or repair processes that counteract UV damage that might be induced concomitantly with MAA accumulation. There are several reasons that our approach might have better distinguished the specific effect of MAAs. First, the MAA content of *G. sanguineum* varied simply as a function of PAR intensity. Sup-

plementation of growth irradiance with UVR was not necessary. Such supplementation might confound comparative studies by inducing other effects besides MAA accumulation. Second, the reported BWFs are the average of four (LL) to five (HL) independent determinations; this enhanced the statistical power of the comparison. Third, photosynthesis was measured at high irradiance under which the consequences of differing BWFs are the most pronounced (Fig. 1).

A simple optical model (Garcia-Pichel 1994) suggested that MAAs are marginally efficient protectants in the size range of dinoflagellates. In most cases, organisms are found to have less than 1% dry mass of protectant. For cells with a $44\text{-}\mu\text{m}$ diameter, the optical model predicts that a 0.5%–1% investment in MAAs would screen 50%–70% of UV radiation. To obtain a more precise estimate of MAA optical protection in *G. sanguineum*, a sunscreen factor (S) was calculated directly from measured absorbance (Fig. 2) using the equations of Garcia-Pichel (1994). We estimated an S of 0.8 for HL cultures, assuming that the background absorbance was equivalent to the LL cells. A similar S was obtained by estimating the increase in UV absorbance from LL to HL cultures using measured MAA concentrations (Table 3) and the maximum extinction coefficient for MAAs ($5.7 \times 10^{-2} \text{L}\cdot\text{g}^{-1}\cdot\mu\text{m}^{-1}$), as reported by Garcia-Pichel (1994). An S of 0.8 implies that the increased MAAs account for an 80% decrease in UV radiation reaching cellular constituents. However, the lowering of UV weight ($\epsilon[\lambda]$) between LL and HL cultures was greater than 80% (Fig. 5), implying that screening performance exceeds both model expectations for $\leq 1\%$ MAA content and direct estimates of screening potential. The calculation of screening factor assumes a homogeneous distribution of MAAs in the cell (Garcia-Pichel 1994). This does appear to be the case for cyanobacteria (Garcia-Pichel and Castenholz 1993), but little is known about intracellular distribution of MAAs in eukaryotes. Targeting of MAAs around cellular structures containing sensitive targets might increase the efficiency of protection. Another possibility is that MAAs are also providing protection through secondary mechanisms, for example, as an antioxidant (Dunlap and Yamamoto 1995). However, such mechanisms would not provide spectrally specific protection and thus would be unlikely to induce the observed changes in BWFs.

Although intercellular distribution of screening compounds might affect the scale of cell sizes over which effective protection is obtained, the general principles of the Garcia-Pichel analysis probably still hold: As cell size becomes smaller, nonoptical defense strategies, such as antioxidants, repair, and reactivation processes, will have better cost/benefit ratios (Raven 1991). Indeed, the contribution of repair needs to be taken into account

for any cell size (Lesser et al. 1994). If there are offsetting processes to damage (as suggested by the observation of negative weights), even incomplete protection from UV radiation might reduce damage enough so that residual biological effects can be completely counteracted by other defenses. Thus, phytoplankton should be expected to have a range of strategies for defending against UV effects, with varying importance of photoprotection and other mechanisms.

CONCLUSIONS

Much progress has been made recently in developing quantitative approaches for estimating UV inhibition of marine photosynthesis (Cullen et al. 1992, Lubin et al. 1992, Neale et al. 1994, Boucher and Prézelin 1996a, Neale et al. 1998a). In principle, these approaches can be used to assess the effect of stratospheric ozone depletion on marine primary productivity (Cullen et al. 1992, Arrigo 1994, Neale et al. 1994, Boucher and Prézelin 1996b, Neale et al. 1998b). However, phytoplankton response to environmental UV radiation is variable (Neale et al. 1998a). Thus, general estimates of the effect of ozone depletion depend on a better understanding of both phenotypic and genotypic variation in UV response. We have shown that the influence of one factor, MAA concentration, can be quantitated through changes in the BWF. This is a first step toward better prediction of how phytoplankton respond to UV radiation on the basis of cellular characteristics and environmental conditions. We suggest that this capability will be further expanded by spectral studies of MAA effects in other species and for other growth conditions and by similar comparative studies to relate changes in the BWF to other photoprotective and repair mechanisms.

This work was supported by grants from the Smithsonian Institution Scholarly Studies program (P.J.N.). A.T.B. was supported with a Smithsonian Postdoctoral Fellowship. John Cullen and Richard Davis provided valuable assistance in the preparation of figures.

Adams, N. L. & Shick, M. J. 1996. Mycosporine-like amino acids provide protection against ultraviolet radiation in eggs of the green sea urchin *Strongylocentrotus droebachiensis*. *Photochem. Photobiol.* 64:149–58.

Arrigo, K. R. 1994. Impact of ozone depletion on phytoplankton growth in the Southern Ocean: large-scale spatial and temporal variability. *Mar. Ecol. Prog. Ser.* 114:1–12.

Balch, W. M. & Haxo, F. T. 1984. Spectral properties of *Noctiluca miliaris* Suriray, a heterotrophic dinoflagellate. *J. Plankton Res.* 6:515–25.

Banaszak, A. T. & Trench, R. K. 1995. Effects of ultraviolet (UV) radiation on marine microalgal-invertebrate symbioses. II. the synthesis of mycosporine-like amino acids in response to exposure to UV in *Anthopleura elegantissima* and *Cassiopea xamachana*. *J. Exp. Mar. Biol. Ecol.* 194:233–50.

Bevington, P. R. 1969. *Data Reduction and Error Analysis for the Physical Sciences*. McGraw-Hill, New York, 336 pp.

Bothwell, M. L., Sherbot, D., Roberge, A. C. & Daley, R. J. 1993. Influence of natural ultraviolet radiation on lotic periphytic diatom community growth, biomass accrual, and species

composition: short-term versus long-term effects. *J. Phycol.* 29: 24–35.

Boucher, N. P. & Prézelin, B. B. 1996a. An *in situ* biological weighting function for UV inhibition of phytoplankton carbon fixation in the Southern Ocean. *Mar. Ecol. Prog. Ser.* 144: 223–6.

——— 1996b. Spectral modeling of UV inhibition of *in situ* Antarctic primary production using a field derived biological weighting function. *Photochem. Photobiol.* 64:407–18.

Buma, A. G. J., van Hanne, E. J., Roza, L., Veldhuis, M. J. W. & Gieskes, W. W. C. 1995. Monitoring UV-B induced DNA damage in individual diatom cells by immunofluorescent thymine dimer detection. *J. Phycol.* 31:314–21.

Carreto, J. I., Carignan, M. O., Dalea, G. & De Marco, S. G. 1990a. Occurrence of mycosporine-like amino acids in the red-tide dinoflagellate *Alexandrium excavatum*: UV-photoprotective compounds? *J. Plankton Res.* 12:909–21.

Carreto, J. I., De Marco, S. G. & Lutz, V. A. 1989. UV-absorbing pigments in the dinoflagellates *Alexandrium excavatum* and *Prorocentrum micans*. Effects of light intensity. In Okaichi, T., Anderson, D. M. & Nemoto, T. [Eds.] *Red Tides: Biology, Environmental Science, and Toxicology*. Elsevier, New York, pp. 333–6.

Carreto, J. I., Lutz, V. A., De Marco, S. G. & Carignan, M. O. 1990b. Fluence and wavelength dependence of mycosporine-like amino acid synthesis in the dinoflagellate *Alexandrium excavatum*. In Graneli, E., Edler, L., Sundström, B. & Anderson, D. M. [Eds.] *Toxic Marine Phytoplankton*. Elsevier, New York, pp. 275–9.

Cleveland, J. S. & Weidemann, A. D. 1993. Quantifying absorption by aquatic particles: A multiple scattering correction for glass fiber filters. *Limnol. Oceanogr.* 38:1321–7.

Coohill, T. P. 1991. Photobiology school. Action spectra again? *Photochem. Photobiol.* 54:859–70.

Cullen, J. J. & Lesser, M. P. 1991. Inhibition of photosynthesis by ultraviolet radiation as a function of dose and dosage rate: results for a marine diatom. *Mar. Biol.* 111:183–90.

Cullen, J. J. & Neale, P. J. 1997. Biological weighting functions for describing the effects of ultraviolet radiation on aquatic systems. In Häder, D.-P. [Ed.] *Effects of Ozone Depletion on Aquatic Ecosystems*. R. G. Landes, Austin, Texas, pp. 97–118.

Cullen, J. J., Neale, P. J. & Lesser, M. P. 1992. Biological weighting function for the inhibition of phytoplankton photosynthesis by ultraviolet radiation. *Science* 258:646–50.

Davidson, A. T., Bramich, D., Marchant, H. J. & McMinn, A. 1994. Effects of UV-B irradiation on growth and survival of Antarctic marine diatoms. *Mar. Biol.* 119:507–15.

Davidson, A. T. & Marchant, H. J. 1994. The impact of ultraviolet radiation on *Phaeocystis* and selected species of Antarctic marine diatoms. In Weiler, C. S. & Penhale, P. A. [Eds.] *Ultraviolet Radiation in Antarctica: Measurements and Biological Effects*. American Geophysical Union, Washington, D.C., pp. 187–206.

Davidson, A. T., Marchant, H. J. & de la Mare, W. K. 1996. Natural UVB exposure changes the species composition of Antarctic phytoplankton in mixed cultures. *Aquat. Micro. Ecol.* 10:299–305.

Dunlap, W. C. & Chalker, B. E. 1986. Identification and quantitation of near-UV absorbing compounds (S-320) in a hermatypic scleractinian. *Coral Reefs* 5:155–9.

Dunlap, W. C., Chalker, B. E. & Oliver, J. K. 1986. Bathymetric adaptations of reef-building corals at Davies Reef, Great Barrier Reef, Australia. III. UV-B absorbing compounds. *J. Exp. Mar. Biol. Ecol.* 104:239–48.

Dunlap, W. C. & Shick, J. M. 1998. Ultraviolet radiation-absorbing mycosporine-like amino acids in coral reef organisms: a biochemical and environmental perspective. *J. Phycol.* 34:418–30.

Dunlap, W. C. & Yamamoto, Y. 1995. Small-molecule antioxidants in marine organisms: antioxidant activity of mycosporine-glycine. *Comp. Biochem. Physiol.* 112b:105–14.

Early, E., Thompson, A., Johnson, C., DeLuisi, J., Disterhoft, P., Wardle, D., Wu, E., Mou, W., Sun, Y., Lucas, T., Mestechkina, T., Harrison, L., Berndt, J., & Hayes, D. 1998. The 1995

- North American interagency intercomparison of ultraviolet monitoring spectroradiometers. *J. Res. Natl. Inst. Stand. Technol.* 103:15–62.
- Falkowski, P. G. & LaRoche, J. 1991. Acclimation to spectral irradiance in algae. *J. Phycol.* 27:8–14.
- Garcia-Pichel, F. 1994. A model for self-shading in planktonic organisms and its implications for the usefulness of ultraviolet sunscreens. *Limnol. Oceanogr.* 39:1704–17.
- Garcia-Pichel, F. & Castenholz, R. W. 1993. Occurrence of UV-absorbing, mycosporine-like compounds among the cyanobacterial isolates and an estimate of their screening capacity. *Appl. Environ. Microbiol.* 59:163–9.
- Garcia-Pichel, F., Wingard, C. E. & Castenholz, R. W. 1993. Evidence regarding the UV sunscreen role of a mycosporine-like compound in the cyanobacterium *Gloeocapsa* sp. *Appl. Environ. Microbiol.* 59:170–6.
- Genty, B., Briantais, J. M. & Baker, N. 1989. The relationship between the quantum yield of photosynthetic electron transport and quenching of chlorophyll fluorescence. *Biochim. Biophys. Acta* 990:87–92.
- Greenberg, B. M., Gaba, V., Canaani, O., Malkin, S., Mattoo, A. K. & Edelman, M. 1989. Separate photosensitizers mediate degradation of the 32-kDa photosystem II reaction center protein in the visible and UV spectral regions. *Proc. Natl. Acad. Sci. USA* 86:6617–20.
- Hannach, G. & Sigleo, A. C. 1998. Photoinduction of UV-absorbing compounds in six species of marine phytoplankton. *Mar. Ecol. Prog. Ser.* in press.
- Helbling, E. W., Chalker, B. E., Dunlap, W. C., Holm-Hansen, O. & Villafañe, V. E. 1996. Photoacclimation of Antarctic marine diatoms to solar ultraviolet radiation. *J. Exp. Mar. Biol. Ecol.* 204:85–101.
- Helbling, E. W., Villafañe, V., Ferrario, M. & Holm-Hansen, O. 1992. Impact of natural ultraviolet radiation on rates of photosynthesis and on specific marine phytoplankton species. *Mar. Ecol. Prog. Ser.* 80:89–100.
- Hirosawa, T. & Miyachi, S. 1983. Inactivation of Hill reaction by long-wavelength radiation (UV-A) and its photoreactivation by visible light in the cyanobacterium, *Anacystis nidulans*. *Arch. Microbiol.* 135:98–102.
- Holm-Hansen, O., Lubin, D. & Helbling, E. W. 1993. UVR and its effects on organisms in aquatic environments. In Young, A. R. et al. [Eds.] *Environmental UV Photobiology*. Plenum, New York, pp. 379–425.
- Kana, T. 1990. Light-dependent oxygen cycling measured by an oxygen-18 isotope dilution technique. *Mar. Ecol. Prog. Ser.* 64:293–300.
- Karentz, D. 1994. Ultraviolet tolerance mechanisms in Antarctic marine organisms. In Weiler, C. S. & Penhale, P. A. [Eds.] *Ultraviolet Radiation in Antarctica: Measurements and Biological Effects*. American Geophysical Union, Washington, D.C., pp. 93–110.
- Karentz, D., Cleaver, J. E. & Mitchell, D. L. 1991a. Cell survival characteristics and molecular responses of Antarctic phytoplankton to ultraviolet-B radiation. *J. Phycol.* 27:326–41.
- Karentz, D., McEuen, F. S., Land, M. C. & Dunlap, W. C. 1991b. Survey of mycosporine-like amino acid compounds in Antarctic marine organisms: potential protection from ultraviolet exposure. *Mar. Biol.* 108:157–66.
- Karentz, D. & Spero, H. J. 1995. Response of natural *Phaeocystis* population to ambient fluctuations of UVB radiation caused by Antarctic ozone depletion. *J. Plankton Res.* 17:1771–89.
- Lesser, M. P. 1996a. Acclimation of phytoplankton to UV-B radiation: oxidative stress and photoinhibition of photosynthesis are not prevented by UV-absorbing compounds in the dinoflagellate *Prorocentrum micans*. *Mar. Ecol. Prog. Ser.* 132:287–97.
- 1996b. Acclimation of phytoplankton to UV-B radiation: oxidative stress and photoinhibition of photosynthesis are not prevented by UV-absorbing compounds in the dinoflagellate *Prorocentrum micans* (Correction). *Mar. Ecol. Prog. Ser.* 141:312.
- Lesser, M. P., Cullen, J. J. & Neale, P. J. 1994. Carbon uptake in a marine diatom during acute exposure to ultraviolet B radiation: relative importance of damage and repair. *J. Phycol.* 30:183–92.
- Lewis, M. R. & Smith, J. C. 1983. A small volume, short-incubation-time method for measurement of photosynthesis as a function of incident irradiance. *Mar. Ecol. Prog. Ser.* 13:99–102.
- Lubin, D., Mitchell, B. G., Frederick, J. E., Alberts, A. D., Booth, C. R., Lucas, T. & Neuschuler, D. 1992. A contribution toward understanding the biospherical significance of Antarctic ozone depletion. *J. Geophys. Res.* 97:7817–28.
- Marchant, H. J., Davidson, A. T. & Kelly, G. J. 1991. UV-B protecting compounds in the marine alga *Phaeocystis pouchetii* from Antarctica. *Mar. Biol.* 109:391–5.
- Neale, P. J., Cullen, J. J. & Davis, R. F. 1998a. Inhibition of marine photosynthesis by ultraviolet radiation: variable sensitivity of phytoplankton in the Weddell-Scotia Sea during the austral spring. *Limnol. Oceanogr.* 43:433–48.
- Neale, P. J., Davis, R. A. & Cullen, J. J. 1998b. Interactive effects of ozone depletion and vertical mixing on photosynthesis of Antarctic phytoplankton. *Nature* 392:585–9.
- Neale, P. J., Lesser, M. P. & Cullen, J. J. 1994. Effects of ultraviolet radiation on the photosynthesis of phytoplankton in the vicinity of McMurdo Station (78°S). In Weiler, C. S. & Penhale, P. A. [Eds.] *Ultraviolet Radiation in Antarctica: Measurements and Biological Effects*. American Geophysical Union, Washington, D.C., pp. 125–42.
- Raven, J. A. 1991. Responses of aquatic photosynthetic organisms to increased solar UV-B. *J. Photochem. Photobiol. B* 9:239–44.
- Richardson, K., Beardall, J. & Raven, J. A. 1983. Adaptation of unicellular algae to irradiance: an analysis of strategies. *New Phytol.* 93:157–91.
- Riegger, L. & Robinson, D. 1997. Photoinduction of UV-absorbing compounds in Antarctic diatoms and *Phaeocystis antarctica*. *Mar. Ecol. Prog. Ser.* 160:13–25.
- Samuelsson, G., Lönneborg, A., Rosenqvist, E., Gustafson, P. & Öquist, G. 1985. Photoinhibition and reactivation of photosynthesis in the cyanobacterium *Anacystis nidulans*. *Plant Physiol.* 79:992–5.
- Schreiber, U. 1994. New emitter-detector-cuvette assembly for measuring modulated chlorophyll fluorescence of highly diluted suspensions in conjunction with the standard PAM fluorometer. *Zeitschrift für Naturforschung* 49c:646–56.
- Schreiber, U., Schliwa, U. & Bilger, B. 1986. Continuous recording of photochemical and nonphotochemical chlorophyll fluorescence quenching with a new type of modulation fluorometer. *Photosyn. Res.* 10:51–62.
- Shibata, K. 1969. Pigments and a UV-absorbing substance in corals and a blue-green alga living in the Great Barrier Reef. *Plant Cell Physiol.* 10:325–35.
- Shick, J. M., Dunlap, W. C., Chalker, B. E., Banaszak, A. T. & Rosenzweig, T. K. 1992. Survey of ultraviolet radiation-absorbing mycosporine-like amino acids in organs of coral reef holothurroids. *Mar. Ecol. Prog. Ser.* 90:139–48.
- Smith, R. C., Baker, K. S., Holm-Hansen, O. & Olson, R. S. 1980. Photoinhibition of photosynthesis in natural waters. *Photochem. Photobiol.* 31:585–92.
- Smith, R. C., Prézelin, B. B., Baker, K. S., Bidigare, R. R., Boucher, N. P., Coley, T., Karentz, D., MacIntyre, S., Matlick, H. A., Menzies, D., Ondrusek, M., Wan, Z. & Waters, K. J. 1992. Ozone depletion: ultraviolet radiation and phytoplankton biology in Antarctic waters. *Science* 255:952–9.
- Stein, J. R., ed. 1973. *Handbook of Phycological Methods: Culture Methods and Growth Measurements*. Cambridge University Press, Cambridge, United Kingdom.
- Stochaj, W. R., Dunlap, W. C. & Shick, J. M. 1994. Two new UV-absorbing mycosporine-like amino acids from the sea anemone *Anthopleura elegantissima* and the effects of zooxanthellae and spectral irradiance on chemical composition and content. *Mar. Biol.* 118:149–56.
- Vernet, M., Brody, E. A., Holm-Hansen, O. & Mitchell, B. G. 1994. The response of Antarctic phytoplankton to ultraviolet radiation: absorption, photosynthesis, and taxonomic composition. In Weiler, C. S. & Penhale, P. A. [Eds.] *Ultraviolet Ra-*

- diation in Antarctica: Measurements and Biological Effects*. American Geophysical Union, Washington, D.C., pp. 143–58.
- Vernet, M., Neori, A. & Haxo, F. T. 1989. Spectral properties and photosynthetic action in red-tide populations of *Prorocentrum micans* and *Gonyaulax polyedra*. *Mar. Biol.* 103:365–71.
- Villafañe, V. E., Helbling, E. W., Holm-Hansen, O. & Chalker, B. E. 1995. Acclimatization of Antarctic natural phytoplankton assemblages when exposed to solar ultraviolet radiation. *J. Plankton Res.* 17:2295–2306.
- Vincent, W. F. & Roy, S. 1993. Solar ultraviolet-B radiation and aquatic primary production: damage, protection and recovery. *Environ. Rev.* 1:1–12.
- Yentsch, C. S. & Yentsch, C. M. 1982. The attenuation of light by marine phytoplankton with specific reference to the absorption of near-UV radiation. In Calkins, J. [Ed.] *The Role of Solar Ultraviolet Radiation in Marine Ecosystems*. Plenum, New York, pp. 691–700.